China Geology 9 (2026) 489−501

China Geology

Journal homepage: http://chinageology.cgs.cn
https://www.sciencedirect.com/journal/china-geology

Cenozoic fault system and its control on gas hydrate accumulation in the eastern Dongsha Island area, northern South China Sea: Insights from high-resolution 3D seismic data

Gang Dong[a, b,*], Yun-bao Sun[a, b,*], Zhi-lei Sun[a, b], Ang Li[a, b], Di Luo[a, b], Qing Li[a, b], Dong Zhang[a, b], Feng Cai[a], Bin Zhai[a, b], Gui-jing Yan[a], Jian-ming Gong[a]

[a] *Technology Innovation Center for Marine Methane Monitoring*, *Ministry of Natural Resources*, *Qingdao Institute of Marine Geology*, *China Geological Survey*, *Qingdao* 266237, *China*
[b] *Laboratory for Marine Mineral Resources*, *Qingdao Marine Science and Technology Center*, *Qingdao* 266237, *China*

ARTICLE INFO

Article history:
Received 28 May 2025
Received in revised form 27 October 2025
Accepted 23 December 2025
Available online 25 February 2026

Keywords:
Gas hydrate
Combustible ice
Clean energy
Cenozoic
Structural features
Fault system
Geodynamic mechanism
Gas migration
Hydrate accumulation
High-resolution 3D seismic data
Geological survey engineering
Eastern Dongsha Island

ABSTRACT

The enrichment and accumulation of natural gas hydrates depend on sufficient gas supply and effective migration pathways. The upward migration of deep thermogenic gases through fault systems is critical for seepage-type hydrate formation. This study aims to elucidate the developmental characteristics of Cenozoic fault systems in the eastern offshore area of Dongsha Island and their influence on natural gas hydrate formation. Utilizing high-resolution 3D seismic data, this study conducted a detailed structural interpretation and seismic attribute analysis to systematically investigate the spatial distribution, developmental stages, and dynamic mechanisms of the Cenozoic fault systems in this region. In addition, this study explored the role of these fault systems in facilitating the migration of deep thermogenic gases to the shallow strata. The study area is dominated by extensional and transtensional normal faults characterized by inherited development and relatively small fault displacements. The Cenozoic strata exhibit a tectonic framework of block-faulted uplift and subsidence with alternating highs and lows. Faults on either side of the central uplift dip in opposite directions and commonly exhibit parallel, step-like patterns. Differences in fault system attitudes were observed between the southern and northern parts of the study area. In the south, fault strikes remained consistent from deep to shallow levels, predominantly trending NE and NEE. In the north, fault strikes varied significantly with depth, transitioning from predominantly NEE in deeper strata to EW and NWW in shallower strata. The study identifies two distinct phases of Cenozoic fault activity: (1) 66–10 Ma, a regional extensional tectonic regime controlled fault development, resulting in the formation of NEE-trending normal faults; (2) 10–2.6 Ma, the Dongsha Movement influenced fault activity, during which EW- and NW–W-trending transtensional faults with dextral strike-slip characteristics developed in the Miocene strata of the northern region. The Cenozoic fault system played a significant positive role in facilitating the migration of deep thermogenic gas to shallow levels, thereby enabling the formation of natural gas hydrates.

©2026 China Geology Editorial Office.

1. Introduction

Natural gas hydrates are a significant potential energy resource that typically occur in disseminated, massive, and vein-like forms in submarine sediments. Hydrate accumulation generally follows three models: Diffusion, seepage, and composite (Collett TS et al., 2009; Bangs NLB et al., 2011; You KH et al., 2015). Among these, seepage-type hydrates, which are characterized by their substantial thickness and concentrated distribution, have become critical targets for energy exploration. The gas sources for seepage-type hydrates are primarily deep thermogenic gas, which migrates upward through geological conduits such as gas chimneys, diapirs, mud volcanoes, and fault systems, ultimately reaching the gas hydrate stability zone (Liang JQ et al., 2019; Wei JG et al., 2019; Ye JL et al., 2019; Zhang W et al., 2019; He YL et al., 2022; Xie ZY et al., 2022; Ren JF et

First author: *E-mail address*: donggang02@163.com (Gang Dong).

* Corresponding author: *E-mail address*: donggang02@163.com (Gang Dong); 646881213@qq.com (Yun-bao Sun).

Literary editor: Li-qiong Jia
doi:10.31035/cg2025120
2096-5192/© 2026 China Geology Editorial Office.

Copyright © 2026 Editorial Office of China Geology. Publishing services by Elsevier B.V. on behalf of KeAi Communications Co. Ltd.
This is an open access article under the CC BY-NC-ND License (http://creativecommons.org/licenses/by-nc-nd/4.0/).

al., 2024). Among these conduits, fault systems play a pivotal role in connecting deep hydrocarbon source rocks to shallow reservoirs (Liu JL et al., 2015; Wei JG et al., 2019). Previous studies have highlighted the importance of sufficient gas supply and fluid migration for gas hydrate accumulation (Wu GX et al., 2007; Shao L et al., 2007; Zhong GJ et al., 2020, 2022). However, the roles of fault systems in controlling gas migration and hydrate accumulation remain unclear. Faults provide migration pathways for deep hydrocarbons and influence the spatial distribution and stability of gas hydrates (Hustoft S et al., 2007; Sun QL et al., 2010; Laurent D et al., 2012; Ostanin I et al., 2012).

The northern slope of the South China Sea, characterized by thick sedimentary sequences, abundant organic matter, and complex tectonic evolution, has emerged as a hotspot for gas hydrate exploration (Shao L et al., 2007; Zhong GJ et al., 2022). Its complex tectonic history has produced a well-developed fault system that significantly influences hydrate accumulation and reservoir formation. Since the Cenozoic, the northern slope of the South China Sea has been dominated by NEE- and EW-trending extensional fault systems that cut through the Mesozoic and Cenozoic strata, providing effective conduits for deep thermogenic gas migration (Lin CS et al., 2007). Previous studies have shown that NEE-trending extensional faults dominate in the Pearl River Mouth Basin, whereas NW- and NWW-trending faults were primarily formed during the Dongsha Movement, exhibiting transtensional characteristics (Li PL, 1994; Ding WW et al., 2010). Notably, some of these faults remain active today, continually influencing deep-gas migration (Briais A et al., 1993; Chen J et al., 2002). In the Jieyang Sag, located to the east of the Dongsha Uplift, right-lateral NE–SW-trending strike-slip faults and left-lateral EW-trending en echelon faults have developed. These differ significantly from the nearly EW- and NWW-trending right-lateral strike-slip fault systems that developed on the western and northern sides of the Dongsha Uplift (Du XD et al., 2021). These structural characteristics have major implications for hydrocarbon migration and hydrate accumulation. Moreover, the extensive distribution of bottom-simulating reflectors (BSRs) identified in the Zhongjianan Basin suggests a close relationship between fault activity, fluid migration, and hydrate accumulation. These BSRs are closely associated with polygonal faults and pockmarks, and reflect active deep-fluid migration (Lu YT et al., 2017, 2021; Liu J et al., 2019). The eastern waters of Dongsha Island, situated at the junction of the Pearl River Mouth Basin and the Chaoshan Depression, have developed multiple stages of extensional and transtensional faults since the Cenozoic. These faults provide favorable conditions for deep fluid migration (Liang JQ et al., 2019; Ye JL et al., 2019).

Although numerous studies have investigated the nature, attitude, controlling factors, and formation mechanisms of fault development on the northern slope of the South China Sea, data quality and resolution limitations persist (Wang XX et al., 2021). Research gaps remain regarding spatiotemporal variations in fault systems across stratigraphic units and their control on deep gas migration and hydrate accumulation.

This study employed newly acquired high-resolution three-dimensional (3D) seismic data complemented by detailed sequence stratigraphy and structural interpretation, combined with seismic attribute analysis, aiming to delineate the spatial distribution and developmental characteristics of the Cenozoic fault system in the eastern waters of Dongsha Island, explore the kinematic mechanisms of faulting, and reveal the role of fault systems in controlling natural gas migration and hydrate accumulation. This study provides valuable scientific insights into the exploration and evaluation of gas hydrates in the northern South China Sea.

2. Regional geological background

The South China Sea is situated in the convergence zone of the Tethys and Pacific tectonic domains, and its formation and evolution have been profoundly influenced by the collision between the Indian and Eurasian plates as well as the northwestward subduction of the Pacific Plate beneath the Eurasian Plate (Li PL, 1993), exhibiting a unique tectonic stress environment and a complex tectonic evolution history (Li SZ et al., 2019; Wang PC et al., 2020; Du XD et al., 2021). Previous studies have revealed that the tectonic evolution of the South China Sea can be divided into three major stages (Wu GX et al., 2007; Wei XD et al., 2011; Xie XN et al., 2019; Wang XX et al., 2021): (1) Rifting stage (65–33 Ma; Late Cretaceous–Early Oligocene), characterized by extensional tectonics, resulting in the formation of rift basins along the continental margin due to crustal stretching and thinning; (2) seafloor spreading stage (33.0–15.5 Ma; Late Oligocene–Early Miocene), during which seafloor spreading was initiated, leading to the generation of oceanic crust and the development of several sedimentary basins; and (3) post-spreading subsidence stage (from 15.5 Ma; Late Miocene to Present), during which tectonic activity gradually stabilized, and the region entered a phase of thermal subsidence. The regional tectonic framework was primarily established with the area transitioning into a thermal subsidence phase accompanied by sedimentary infilling (Zhou D et al., 1995; Huang CY et al., 2001; Zhao SJ et al., 2012).

Cenozoic sedimentary basins along the northern margin of the South China Sea have undergone significant changes in their depositional environments and structural characteristics owing to tectonic evolution. For example, the sedimentary environment of the Southwest Taiwan Basin has transitioned from terrestrial and transitional deposits to semi-deep and deep marine deposits since the Paleocene (Ding WW et al., 2004; Wang XX et al., 2021). The Pearl River Mouth Basin (PRMB)—a key Cenozoic extensional hydrocarbon-bearing basin in the northern South China Sea—has undergone complex tectonic evolution, characterized by unconformities, stratigraphic hiatuses, fault activity, and magmatism, which

can be further classified into five major tectonic events (Li PL, 1993).

The Dongsha Uplift is a prominent structural unit in the eastern part of the central uplift zone of the PRMB. Geographically, it is bordered by the Taixi and Southwest Taiwan basins to the east, the Chaoshan Depression to the south, the Zhu Ⅱ Depression to the southwest, the Panyu Low Uplift to the west, and the Zhu Ⅰ Depression to the north. The tectonic evolution of the Dongsha Uplift can be divided into five principal stages: (1) Cretaceous compression stage: Intense compressional deformation occurred due to regional tectonic stresses; (2) Paleocene–Early Oligocene extensional rift stage: A transition from compression to extension led to the formation of large-scale extensional faulted basins controlled primarily by normal faulting; (3) Late early Oligocene uplift and erosion stage: Regional uplift resulted in erosion and denudation, which caused stratigraphic hiatuses and unconformities; (4) Late Oligocene–Miocene rapid post-rift subsidence stage: Continuous basin subsidence occurred, accompanied by enhanced deep-water environments and accelerated sedimentary infilling; and (5) Late Miocene block uplift and subsidence stage: The tectonic regime gradually stabilized, although localized differential uplift and subsidence persisted due to continuous fault activity.

The five tectonic evolutionary stages of the Dongsha Uplift represent a manifestation of the three major regional tectonic evolutionary stages of the South China Sea within a local structural unit. This evolutionary process inherited the regional tectonic characteristics of the northern continental margin of the South China Sea and exhibited significant local uniqueness. The five-stage division scheme corresponded well to the major regional unconformities revealed by the seismic data (e.g., T_g, T_{70}, T_{60}, and T_{30}). These interfaces can be traced and correlated continuously across the Dongsha Uplift, indicating that the five-stage evolutionary model exhibits regional tectonic consistency. For example, the T_{70} unconformity (corresponding to the South China Sea Movement) marks the entry of the northern continental margin basins of the South China Sea, including the Pearl River Mouth Basin, into the developmental stage of sag formation; while the T_{30} interface (related to the Dongsha Movement) records tectonic evidence of local uplift during the block uplift and subsidence stage. Within this tectonic evolutionary framework, the differences between the Dongsha Uplift and adjacent secondary structural units can be reasonably explained. Taking the block uplift and subsidence stages as an example, the elevated parts of the Dongsha Uplift experienced erosion owing to tectonic uplift, whereas the peripheral slope zones and adjacent sags continued to subside, receiving thicker sedimentary deposits. This spatial differentiation in tectonic-sedimentary responses highlights the local tectonic uniqueness of the Dongsha Uplift, shaped by a regional dynamic background.

Sufficient gas sources and effective fluid migration pathways are critical factors in controlling the formation of natural gas hydrate accumulations. The northern slope of the South China Sea hosts several large and medium-sized Meso-Cenozoic sedimentary basins, such as the Pearl River Mouth Basin and the Qiongdongnan Basin. These basins are characterized by high sedimentation rates and sedimentary thicknesses of up to 11 km, providing favorable geological conditions for hydrocarbon and hydrate accumulation. Petroleum geological studies indicate that the Meso–Cenozoic sedimentary basins on the northern slope of the South China Sea feature well-developed mudstone sequences with a high organic matter abundance, containing multiple sets of source rocks and an ample supply of deep pyrolytic gas (Zhong GJ et al., 2020, 2022). Drilling data further confirm the presence of marine Mesozoic strata in the northeastern South China Sea. As an important tectonic unit in this region, the Chaoshan Depression underwent multiple phases of tectonic evolution during the Mesozoic, with depositional environments including marine systems (shallow marine, bathyal, and abyssal facies) and continental systems (fluvial and lacustrine facies). Among these, the Upper Triassic–Jurassic sequences comprise thick mudstones. These source rocks are relatively proximal to the sediment sources and exhibit high organic-matter abundance, representing the principal intervals for Mesozoic source-rock development in the offshore area. They possess substantial hydrocarbon-generation potential and show promise for oil and gas exploration. Drilling results from Well LF35-1-1 reveal that the Middle–Upper Jurassic in the Chaoshan Depression contains organic-rich marine strata, further corroborating the development characteristics of source rocks in this area (Shao L et al., 2007; Wu GX et al., 2007). The spatial coexistence of shallow natural gas hydrates and deep petroleum-bearing systems on the northern slope of the South China Sea forms a structural model characterized by "hydrates above, hydrocarbons below". This configuration has significant implications for the coordinated exploration and comprehensive development of natural gas hydrates and conventional oil and gas resources (Liu JL et al., 2015; Zhong GJ et al., 2018).

The study area is located in the northeastern part of the Chaoshan Depression within the PRMB, near the Southwest Taiwan Basin and Dongsha Uplift, with structural trends generally oriented NE–SW (Fig. 1). The Chaoshan Depression is a typical Mesozoic residual depression situated along the northern margin of the South China Sea (Li CF et al., 2008; Long GS et al., 2011; Zhong GJ et al., 2022). It covers an area exceeding 37000 km^2, with water depths ranging from 300 m to 2000 m. Studies have shown that this region is predominantly characterized by extensional faults, which penetrate both Cenozoic and Mesozoic strata, providing essential pathways for the migration of deep hydrocarbons and fluids (Wei XD et al., 2011).

3. Materials and methods

In this study, high-resolution 3D seismic data were acquired by the Research Vessel (R/V) *Haiyang Dizhi Jiuhao*.

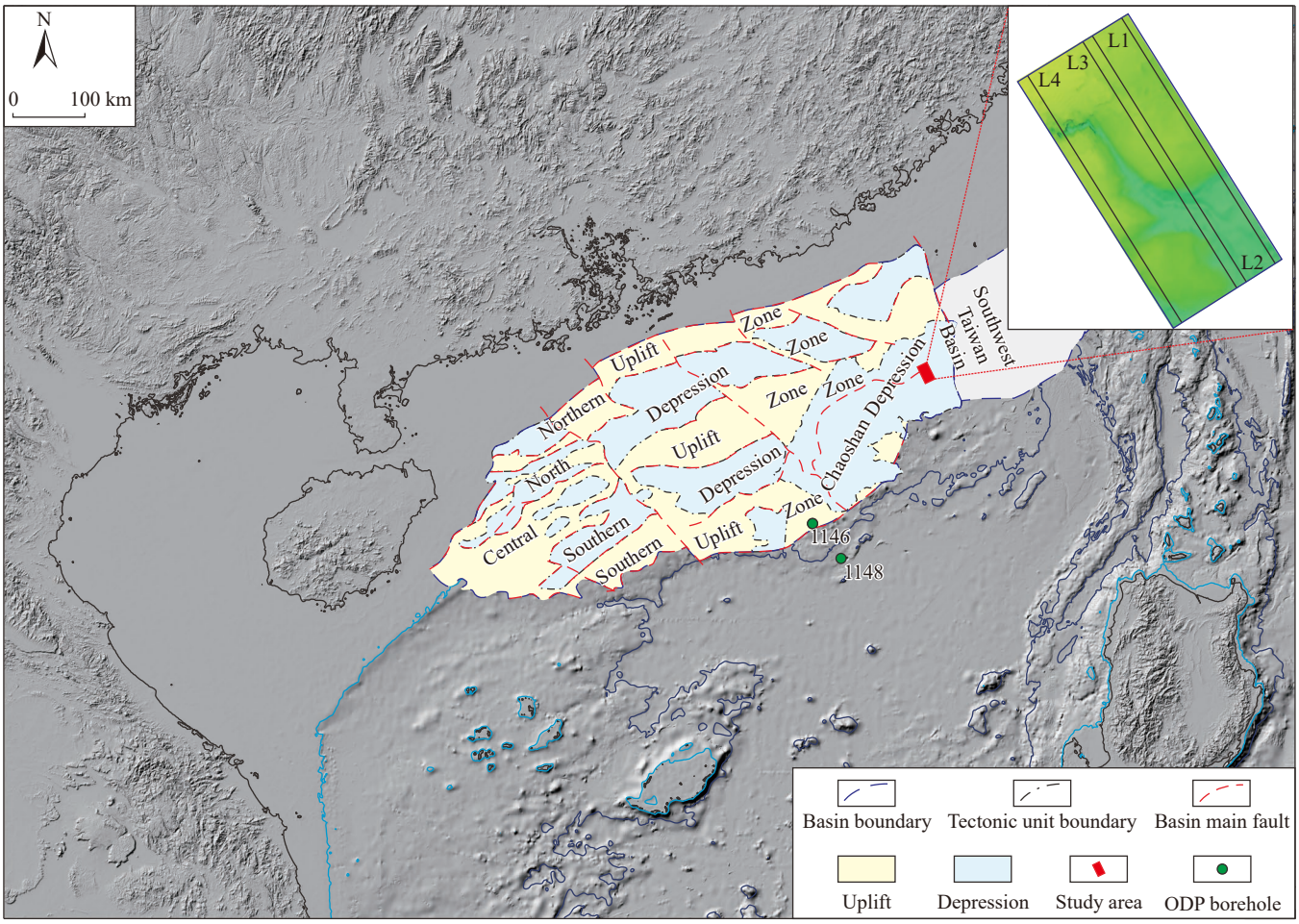

Fig. 1. Structural zoning of the Pearl River Mouth Basin and location of the study area. L1, L2, L3 and L4 are the locations of the profiles in Fig. 3.

Additionally, two-dimensional (2D) seismic data, well logs from the China National Offshore Oil Corporation (CNOOC), and borehole data from the Ocean Drilling Program (ODP) were used to validate the seismic sequence stratigraphy.

The 3D seismic data were acquired using two parallel 240-channel seismic streamers, with a channel spacing of 12.5 m and a temporal sampling interval of 1 ms. An air gun array was used as the seismic source, with a shot interval of 25 m and a recording length of 8 s, ensuring effective coverage of both deep and shallow stratigraphic reflections. Conventional seismic data processing procedures include the following steps: (1) Noise suppression; (2) multiple attenuations; (3) high-precision velocity analysis; and (4) pre-stack time migration imaging. To meet the specific requirements of gas hydrate research, high-fidelity processing techniques have been employed to enhance the signal-to-noise ratio of shallow seismic reflections through pre-stack preprocessing and high-precision velocity modeling.

Based on processed 3D seismic data, fault and sequence interpretations were conducted in *Petrel*, identifying major seismic sequence boundaries (T_1, T_2, T_3, T_4, T_6, T_g). To analyze the spatial distribution of faults, variance-based attribute extraction was applied to delineate fault planes, and bidirectional rose diagrams were generated to illustrate fault orientations. The tectonic mechanisms responsible for fault development were determined through an integrated analysis of regional tectonic evolution and stress-field patterns.

4. Seismic data interpretation

4.1. Seismic sequences

Previous studies have extensively investigated the seismic sequences of the Pearl River Mouth Basin using seismic and drilling data acquired by the CNOOC and borehole data from the ODP (sites 1146 and 1148). Several key seismic reflection interfaces have been identified based on their seismic reflection characteristics, and their correlations with major tectonic events in the northern South China Sea have been discussed (Lüdmann T et al., 2001). This study builds upon the established seismic sequence interpretation framework (Li PL, 1993; Cai ZR et al., 2010; Zhao SJ et al., 2012; Xie ZY et al., 2017; Gao YD et al., 2021; Wang XX et al., 2021; Gao YD et al., 2024) and integrates the seismic reflection characteristics and sequence boundary markers identified from both 2D and 3D seismic data within the study area. A Cenozoic seismic sequence stratigraphic framework was established for the study area (Fig. 2). Six major seismic sequence boundaries were identified in the seismic profiles (T_1, T_2, T_3, T_4, T_6, and T_g). Based on these boundaries, six

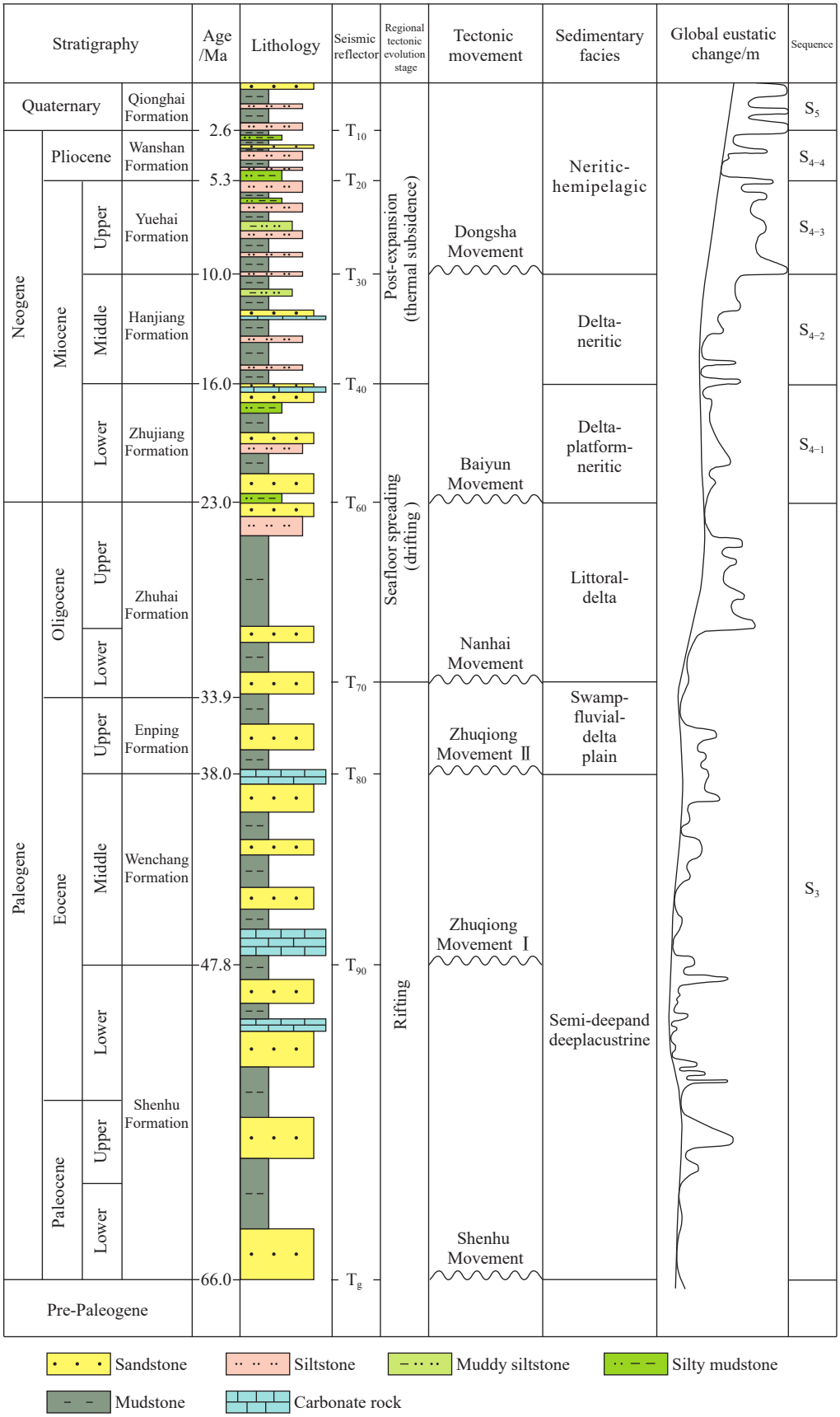

Fig. 2. Seismic sequence division of the study area.

principal seismic sequences were delineated and named from top to bottom: S_5, S_{4-4}, S_{4-3}, S_{4-2}, S_{4-1}, and S_3.

The S_3 sequence corresponds to the Paleogene and records a transitional process from marine regression to continental sedimentation. During this period, large-scale regression provided an abundant sediment supply, promoting the

development of widely distributed fluvial deltaic and fan delta systems. The S_{4-1} sequence corresponds to the Lower Miocene and reflects a major marine transgression. It is characterized by high-frequency, low-amplitude, overlapping depositional sequences predominantly distributed along shelf-edge slope breaks and deep-sea basins, with local occurrences of overlapping patterns. Above the slope break, thin transgressive deposits dominated by mudstone were observed, whereas slope fan systems developed below the slope break. The depositional cycles were primarily controlled by sea-level rise. The S_{4-2} sequence corresponds to the Middle Miocene and is dominated by highstand deposits, with highstand progradation evident on some seismic profiles. It is predicted that this sequence mainly comprises mud-dominated deposits within the study area. The S_{4-3} sequence corresponds to the Upper Miocene, and its lower part comprises high-frequency, medium- to high-amplitude, continuous depositional sequences that partially fill the topography formed by the preceding highstand sequence. Terrestrial sediments prograded significantly towards the marine basin. From the late transgressive to the early regressive stage, highstand progradation deposits developed along the slope break, with local incised channels. Studies indicate that the Dongsha Submarine Canyon underwent its most pronounced development during the Late Miocene (Wang XX et al., 2021). The S_{4-4} sequence corresponds to the Pliocene and exhibits a distinct angular unconformity and seaward-migrating depositional architecture, reflecting a relative sea-level fall. During this stage, the shelf-edge slope break became prominent with steeply inclined strata along the continental slope. Large-scale incised channels are formed under specific triggering conditions. Slope fans and turbidite fan deposits developed along the slope toe and basin floor, respectively. The S_5 sequence corresponds to the Quaternary and is characterized by high-angle shelf-edge slope foresets, with its basal boundary represented by a prominent erosional surface or low-angle unconformity overlain by infillings of mud-rich incised valleys.

4.2. Fault characteristics

4.2.1. Fault development pattern in vertical profiles

Based on a detailed interpretation of high-resolution 3D seismic data, the faults in the study area predominantly exhibit extensional structural characteristics. Normal faults and transtensional normal faults controlled by regional extensional and transtensional stress fields have mainly developed since the Cenozoic, whereas thrust faults have not been observed. Faults with significant horizontal extent generally exhibit inherited characteristics, with activity spanning the entire Cenozoic era. Overall, most faults exhibited small fault throws (vertical displacements usually less than 20 m), resulting in limited deformation of the stratigraphic units.

The Cenozoic strata within the study area were influenced by regional extensional processes, resulting in a structural pattern characterized by block faulting, uplift, and alternating depressions (Fig. 3). Seismic profiles revealed that the study area is primarily located within a faulted uplift zone, with higher elevations in the central part and lower elevations on both sides controlled by extensional normal faults (Fig. 3). The faults on both sides of the central uplift exhibited opposing dip directions and were inclined towards the centers of the adjacent depressions. These two sets of oppositely dipping faults intersect and mutually truncate at the central uplift, forming a characteristic X-shaped conjugate fault pattern, a typical structural feature in extensional regimes (Bao X et al., 2010). On the seaward side (southeastward), a major fault (Fault F in Fig. 3) developed along the inclined margin of the uplift, extending through both the shallow and deep strata. This fault displays extensive vertical and horizontal continuity, likely evolving through continuous development along the earlier fault slip planes. Faults on the seismic profiles were predominantly arranged in parallel or step-like patterns, with local occurrences of negative flower structures (Line L1 in Fig. 3), indicating the influence of transtensional stress fields. The faults exhibit pronounced inheritance in their vertical extension (Fault F in Fig. 3), suggesting that later-stage faults continue to develop along pathways established by earlier faults.

4.2.2. Horizontal distribution characteristics of faults

Based on the fault distribution map in the horizontal plane, significant differences in fault geometries are evident across various parts and strata of the study area. By using the central line of the study area as a boundary (indicated by the blue dashed line in Fig. 4), the region can be divided into northern and southern sections. The northern fault system is predominantly composed of normal faults dipping northward, NNE, and NNW. The fault strike exhibits considerable variation with depth. At deeper stratigraphic levels, such as T_g (Paleogene basal boundary) and T_{60} (Paleogene top boundary), fault strikes are primarily oriented NEE. However, at shallower levels, such as T_{40} (Middle Miocene basal boundary) and T_{30} (Middle Miocene top boundary), fault strikes shift to EW and NWW. In contrast, the southern fault system is mainly characterized by normal faults dipping to the SSE (Fig. 4). The fault strikes in this region show minimal variation with depth, generally maintaining NE and NEE trends.

The variations in fault strikes are closely related to the evolution of the regional stress field during different geological periods. The southern region experienced a relatively stable extensional stress regime from the Paleogene to the Miocene, resulting in consistent fault strikes. Conversely, the northern region was primarily influenced by an extensional stress regime during the Paleogene, forming NE–E-trending normal faults. However, during the Miocene, the shallow strata were influenced by a transition from extensional to transtensional stress regimes. This shift in stress characteristics and direction significantly impacted the spatial development of faults. This stress regime shift is manifested as strike-slip characteristics on the horizontal

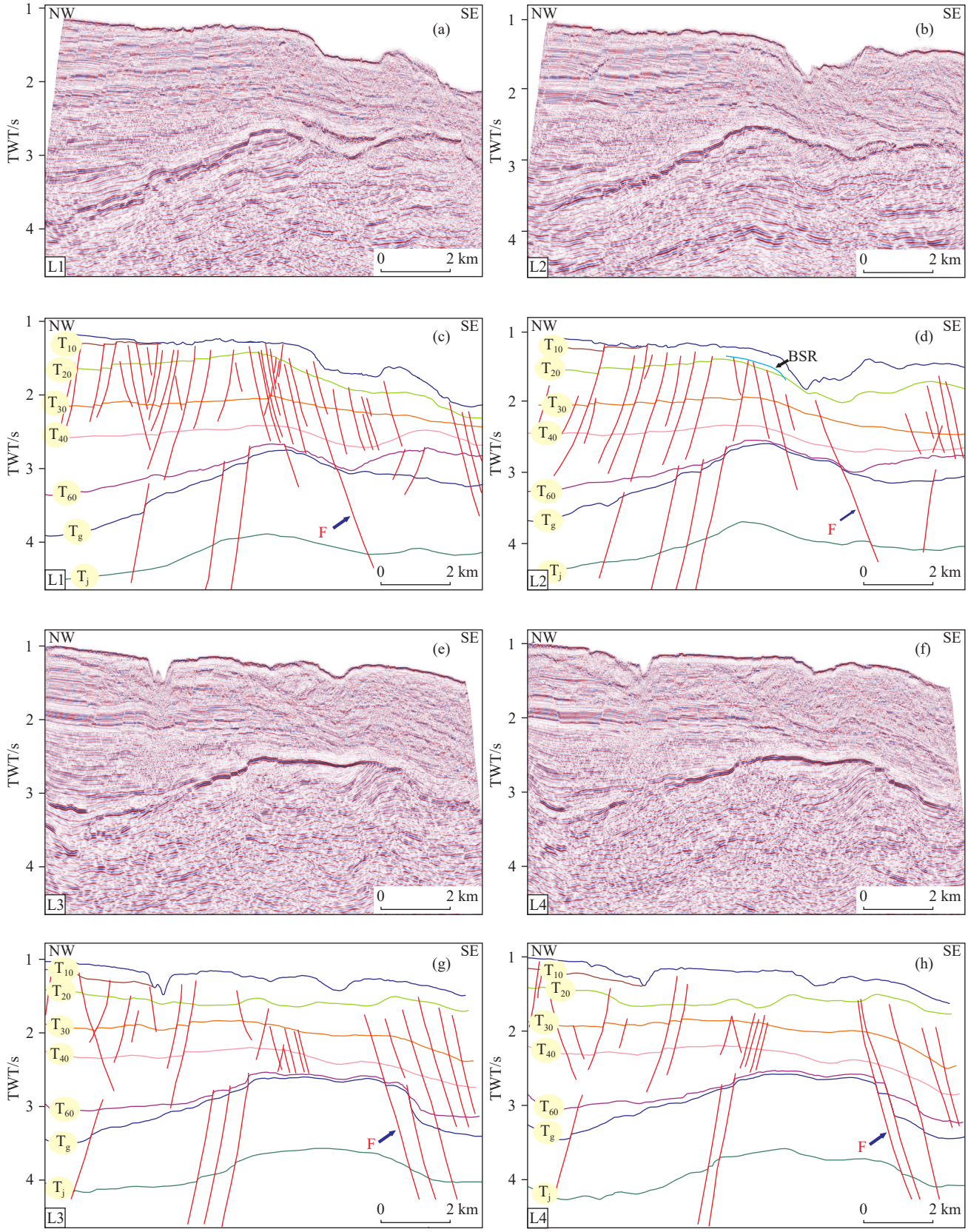

Fig. 3. Seismic profile interpretation results (see Fig.1 for profile location). The colored solid lines indicate the interpreted seismic horizons. T_{10}, T_{20}, T_{30}, T_{40} and T_{60} correspond to the basal boundaries of the Quaternary, Pliocene, Upper Miocene, Middle Miocene, and Lower Miocene, respectively, whereas T_g and T_j correspond to the basal boundaries of the Paleogene and Jurassic. The red solid lines indicate faults.

plane (Fig. 5). In seismic profiles, negative flower structures related to strike-slip motion are observed (Line L1 in Fig. 3), reflecting distinct differences in tectonic evolution between the northern and southern parts of the study area.

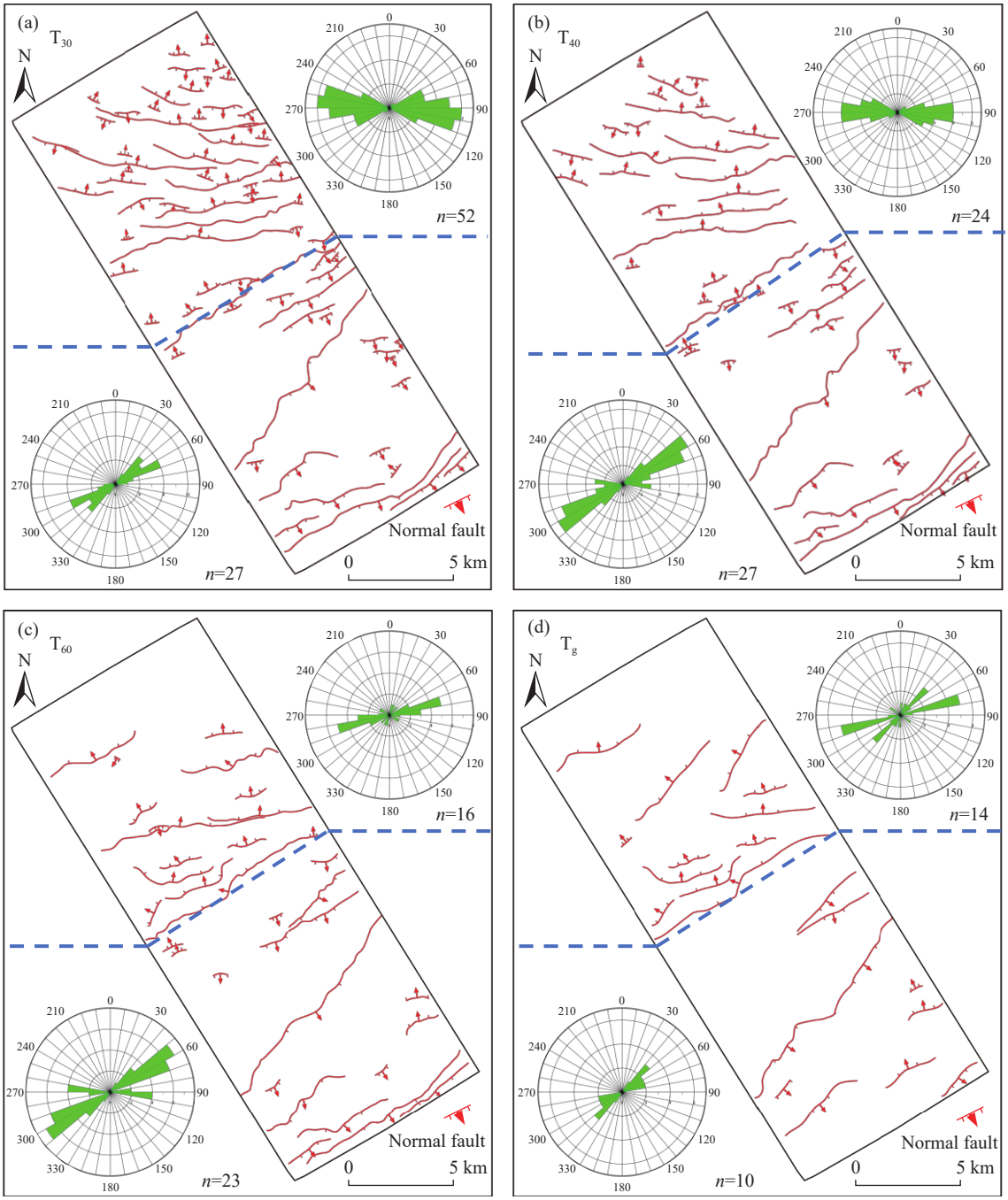

Fig. 4. Fault occurrence and spatial distribution characteristics shown in the ichnography of faults on seismic horizons T_{30} (a), T_{40} (b), T_{60} (c), and T_g (d), respectively. The corresponding rose diagrams show the statistical characteristics of fault strikes on each horizon. "*n*" represents the number of faults. The blue dashed line marks the north–south boundary of the study area.

5. Discussion

5.1. Dynamics of fault development

From the spatial distribution of faults, it is evident that the study area was continuously subjected to regional extensional and transtensional tectonic stresses during the Cenozoic, resulting predominantly in normal and transtensional normal faults, with no significant development of reverse faults. These extensional faults remained active throughout the Cenozoic, with some cutting through both the Cenozoic and Mesozoic strata. Although the overall tectonic regime of the study area is extensional, the orientation and sources of the stress fields have evolved over geological time, leading to spatial and stratigraphic variations in the fault development characteristics. Based on the fault development patterns and their correspondence with regional tectonic events, the Cenozoic fault activity in the study area was divided into two main stages: 66–10 Ma (Paleogene to Late Middle Miocene) and 10–2.6 Ma (Late Middle Miocene to Late Pliocene).

5.1.1. Stage One (66–10 Ma): Fault development under a regional extensional tectonic regime

The first stage of Cenozoic fault activity (66–10 Ma)

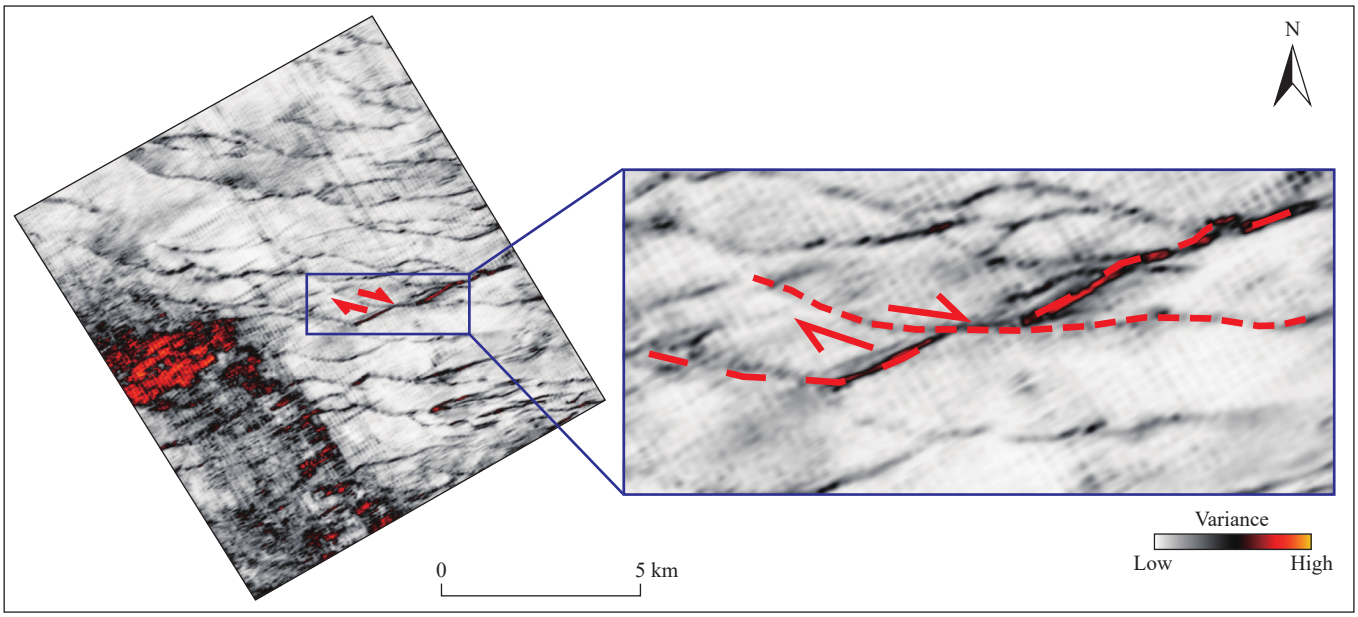

Fig. 5. Time slice (TWT=1463 ms) of variance attributes near the Miocene top boundary (T_{20}) and fault combination characteristics.

includes the rifting phase from the Late Cretaceous to Early Oligocene (65–33 Ma) and the seafloor spreading phase from the Late Oligocene to Early Miocene (33.0–15.5 Ma), both of which occurred within a regional extensional tectonic setting (Zhou D et al., 1995; Huang CY et al., 2001; Zhao SJ et al., 2012). This stage witnessed several major tectonic events, including the Shenhu Movement, the Zhuqiong Movements Ⅰ and Ⅱ, the South China Sea Movement, and the Baiyun Movement. The Shenhu Movement (Late Cretaceous to Early Paleocene) marked the onset of passive continental margin development in the northern South China Sea (Cai ZR et al., 2010). During this time, major basins such as the Pearl River Mouth Basin developed NNE–NE-trending faulted depressions accompanied by NW-trending conjugate faults, establishing a tectonic framework characterized by north–south zoning and east–west blocking (Li PL, 1993). The Zhuqiong Movements Ⅰ (Early to Middle Eocene, ca. 48 Ma) and Ⅱ (Middle to Late Eocene, ca. 38 Ma) triggered the second and third rifting episodes, accompanied by faulting and localized magmatic activity. However, no significant magmatic features were observed in the study area, indicating a limited impact from the dominant NE- and EW-trending faults. The South China Sea Movement (the latest Eocene to Early Oligocene) marked the initiation of seafloor spreading, during which the study area entered a phase of depression development, accompanied by regional uplift and erosion, and dominated by NEE–EW-trending faults (Lin CS et al., 2007). The Baiyun Movement was most pronounced in the Baiyun Sag of the Pearl River Mouth Basin, but was relatively weak in the vicinity of the study area (Du XD et al., 2021). During this stage, the fault activity in the study area was highly consistent with regional tectonic patterns, with both the northern and southern sectors dominated by NE- and NEE-trending normal faults. These fault characteristics are primarily controlled by the extensional stress regime formed jointly by the subduction and rollback of the Pacific Plate along the South China margin and collision between the Indian and Eurasian plates (Ren JS et al., 1990; Li PL 1993; Xia B et al., 2004; Lin CS et al., 2007; Cai ZR et al., 2010).

5.1.2. Stage Two (10–2.6 Ma): Localized transtensional evolution driven by the Dongsha Movement

The second stage of Cenozoic fault activity (10–2.6 Ma) occurred during the post-spread thermal subsidence phase of the South China Sea (15.5 Ma to present). The dominant tectonic event of this stage was the Dongsha Movement (approximately 10–5 Ma), a localized tectonic episode that primarily affected the Dongsha Uplift and Chaoshan Depression (Lin CS et al., 2007). The Dongsha Movement is characterized by block faulting, fault development, and frequent magmatic activity (Zhao SJ et al., 2012; Fan CY et al., 2017; Xie ZY et al., 2017; Sun QL et al., 2020), resulting in the erosion of strata in uplifted areas and the absence of Miocene and parts of Pliocene sequences. During this period, numerous EW- and NWW-trending transtensional faults with minor right-lateral strike-slip components developed in the study area (Fig. 5). The driving force behind the Dongsha Movement was the subduction of the South China Sea Plate beneath the Philippine Plate along the Manila Trench (Wang XX et al., 2021). Subduction and thermal subsidence of the oceanic crust placed the northern margin of the South China Sea in an extensional setting. Magmatic underplating forms a high-velocity layer in the lower crust, disrupting crustal isostasy and inducing the uplift of the upper crust (Zhao SJ et al., 2012). The impact of the Dongsha Movement was particularly significant in the northern part of the study area, where numerous transtensional faults developed within the Miocene strata. In contrast, such faults are less developed in the southern region, indicating distinct spatial variations (Fig. 4).

5.1.3. Basis for the division of fault activity stages

The use of 10 Ma as the boundary between the two fault

activity stages is primarily based on the initiation of the Dongsha Movement and its significant role in reshaping the tectonic framework of the study area. Seismic interpretation results (Figs. 3, 4) show that after the late Middle Miocene (ca. 10 Ma), fault strikes in the northern area shifted from NEE-trending to EW- and NWW-trending, accompanied by enhanced transtensional features. This timing aligns with the Dongsha Movement (10–5 Ma) (Lin CS et al., 2007; Zhao SJ et al., 2012). In contrast, the five-stage tectonic division of the Dongsha Uplift focuses more on the macroscopic processes of sedimentary subsidence and uplift, while the two-stage division of fault activity emphasizes changes in the stress field and their direct influence on fault development. The difference between these staging schemes reflects the variation in research scales and objectives and does not imply a direct correspondence. Future studies incorporating more seismic and drilling data are needed to further validate the precision of the 10 Ma boundary and its correlation with regional tectonic events.

5.2. Tectonic control of fault systems on gas hydrate formation

The formation of natural gas hydrates relies on the migration of methane and other gases into the gas hydrate stability zone (GHSZ), where they combine with water under suitable pressure and temperature conditions. An abundant gas supply is a prerequisite for hydrate accumulation. In sedimentary strata, gas sources primarily include biogenic methane generated from shallow degradation of organic matter and thermogenic gas derived from the thermal cracking of deeper hydrocarbon source rocks (Zhong GJ et al., 2020). Thermogenic gas from deeper layers migrates upward through fluid migration conduits, such as faults and gas chimneys, eventually forming hydrates within the GHSZ. Fault zones are typically associated with elevated gas fluxes and are regarded as key regions for hydrate accumulation. On the northern continental slope of the South China Sea, the study area is underlain by thick Cenozoic mudstone sequences rich in organic matter, forming multiple sets of high-quality source rocks and providing a robust supply of thermogenic gas (Zhong GJ et al., 2022). Previous studies have indicated that both continental and transitional facies deposits in the early evolution of the Pearl River Mouth Basin reached the threshold for hydrocarbon generation (Xie XN et al., 2011). In the deep-water domains of the basin, elevated geothermal gradients have enabled marine source rocks of the Miocene age to reach thermal maturity (Tang XY et al., 2014). Against this geological backdrop, fault systems play a fundamental role in controlling gas migration and hydrate accumulation processes.

5.2.1. Role of faults in forming fluid migration pathways

The Cenozoic fault system in the study area developed under the influence of regional extensional and transtensional stress regimes, resulting in dense networks of normal and strike-slip normal faults. These faults are arranged in parallel and en echelon configurations in cross-section. At the central uplift zones, intersecting fault sets with opposing dips form X-shaped conjugate fault patterns, greatly enhancing the structural connectivity of the fault network (Fig. 3). Some faults penetrate both Cenozoic and Mesozoic strata, directly linking deep source rocks with shallower reservoirs and forming efficient vertical migration pathways. Most of these faults are steeply dipping, favoring rapid vertical migration of gas along the fault planes. Seismic data reveal a high fault density in the area, particularly along the flanks of the central uplift, where fault clustering improves the spatial efficiency of gas flux (Fig. 4). The variation in fault attitude from deep to shallow strata in the northern study area enhances the extension and interconnection of faults from different strata and tectonic phases. This likely significantly improves the connectivity of fluid migration pathways, creating dominant conduits for the upward migration of deep fluids. This process provides critical conditions for channeling deep thermogenic gases into the shallow gas hydrate stability zone and subsequently facilitates the accumulation of seepage-type hydrates. Drilling data, such as from Well LF35-1-1, confirm the presence of organic-rich Jurassic marine mudstones (Middle–Upper Jurassic) within the Chaoshan Depression, with thicknesses of up to 500–535 m (Shao L et al., 2007; Wu GX et al., 2007), providing a substantial source for thermogenic gas. These lines of evidence demonstrate that the fault system has constructed an effective migration network that facilitates upward gas transport into shallower strata (Fig. 6).

5.2.2. Fault-induced optimization of gas hydrate accumulation conditions

Fault systems control gas migration and modify the reservoir–seal configuration in shallow strata, thereby enhancing conditions for hydrate accumulation. The tectonic activity has shaped a block-faulted structural framework characterized by alternating uplifts and depressions (Fig. 3). The depressions adjacent to the central uplifts serve as accommodation spaces for sediment infill, promoting the deposition of porous media suitable for hydrate storage. Seismic sequence stratigraphic analysis revealed the development of slope and turbidite fans in the Upper Pliocene (S_{4-4}) and Quaternary (S_5) sequences (Fig. 2), where coarse-grained sediments with high porosity provided excellent reservoir conditions. Concurrently, fault-related uplift and erosional truncation facilitated the deposition of overlying fine-grained mudstones, which served as effective seals, trapping migrating gas and preventing its release. Previous studies have shown that the Dongsha submarine canyon system experienced intense development during the Late Miocene (Wang XX et al., 2021), with associated turbidity currents contributing to favorable reservoir-seal assemblages within the hydrate stability zone. Seismic data also indicate the presence of gas chimneys and diapiric structures related to faults in the shallow subsurface (Zhang W et al., 2019), highlighting the role of faulting in promoting gas concentrations within the GHSZ. Moreover, zones of high gas

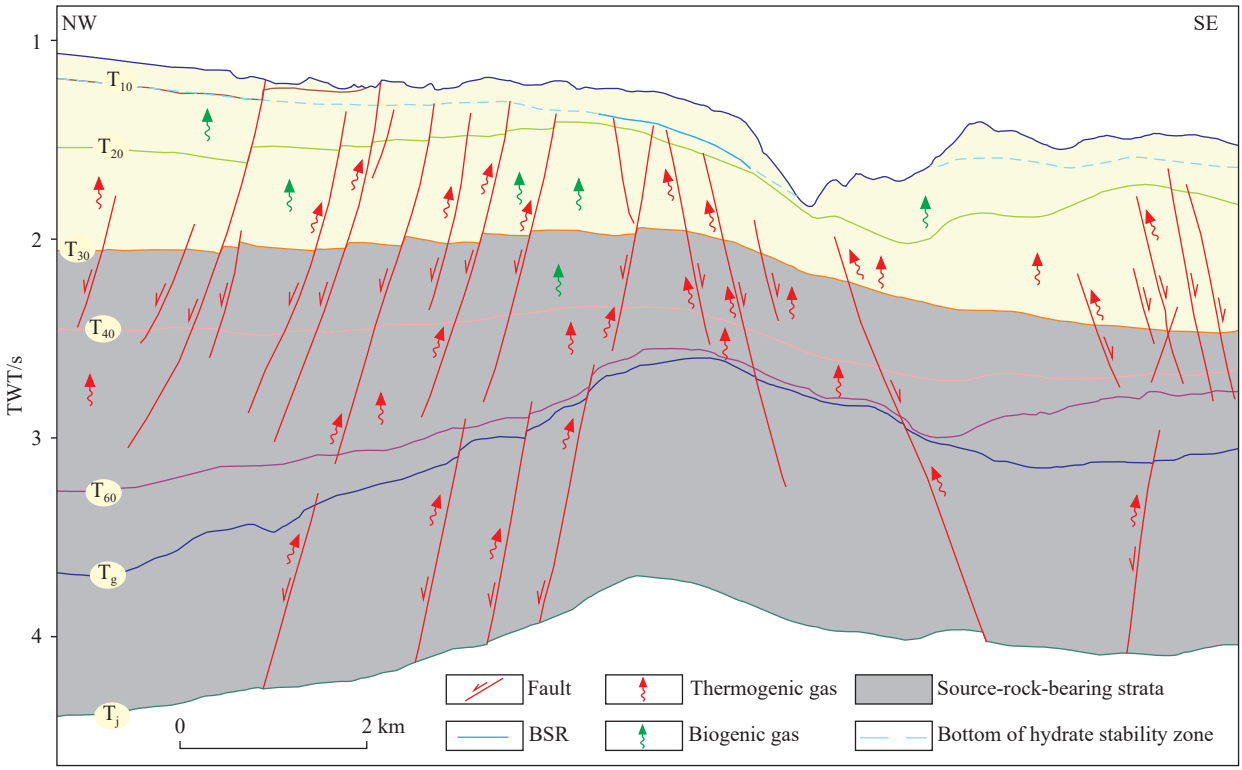

Fig. 6. Gas migration and hydrate accumulation model of the study area.

flux near faults are commonly associated with massive gas hydrate deposits, suggesting that fault systems contribute significantly to leakage-type hydrate accumulation.

6. Conclusions

(i) Since the Cenozoic era, the Dongsha Island area has been subjected to a combination of regional extensional and transtensional tectonic stress fields, resulting in the dominant development of extensional and transtensional normal faults with no evidence of reverse faulting. Large-scale faults with significant lateral continuity exhibited pronounced structural inheritance characteristics, with fault activity persisting throughout the Cenozoic. Most faults are characterized by small vertical displacements (typically less than 20 m), indicating limited structural reworking of the strata. The overall Cenozoic structural configuration is dominated by block faulting and alternating uplift–depression patterns. On both flanks of the central uplift, the faults dip in opposite directions and intersect within the uplift zones, forming classic X-shaped conjugate fault systems. In this profile, faults are commonly arranged in parallel or step-like configurations and locally display negative flower structures indicative of transtensional stress regimes.

(ii) There are distinct differences in fault geometry between the northern and southern parts of the Dongsha Island. The northern fault system is dominated by normal faults dipping northward, NNE and NNW, whereas the southern part is mainly controlled by SSE-dipping normal faults. In the south, fault strikes consistently range from NE to NEE, from the deep to shallow levels. In contrast, fault strikes in the north vary significantly with depth. Deeper structural horizons, such as T_g (base of the Paleogene) and T_{60} (top of the Paleogene), are mainly oriented NEE. However, at shallower horizons (T_{40}–base of the Middle Miocene and T_{30}–top of the Middle Miocene), fault strikes shift to EW and W–NW. These differences reflect variations in the evolution of regional stress fields: The southern region has been continuously influenced by extensional stress from the Paleogene to the Miocene, whereas the northern region experienced primarily extensional stress during the Paleogene, transitioning to transtensional regimes in the Miocene, particularly in shallow stratigraphy.

(iii) Cenozoic faulting of the study area can be divided into two main phases: 66–10 Ma (Paleogene to Late Middle Miocene) and 10–2.6 Ma (Late Middle Miocene to Late Pliocene). The first phase occurred under a regional extensional tectonic setting, with fault development consistent with the broader tectonic framework of the South China Sea. During this phase, both northern and southern regions were dominated by NE- and NEE-trending normal faults. The second phase was influenced by the Dongsha Movement, during which the Miocene strata developed numerous EW- and W–NW-trending transtensional faults with right-lateral strike-slip components. The impact of this tectonic phase is more pronounced in the northern area, where such faults are common, whereas they are rarely observed in the south. The fault system serves as an effective conduit connecting deep hydrocarbon sources with the shallow gas hydrate stability zone, and plays a critical role in the migration, accumulation, and entrapment of natural gas hydrates.

CRediT authorship contribution statement

Gang Dong conceived of the study. Material preparation, data collection and analysis, fault interpretation, and figure and table preparation were also performed by Gang Dong. Seismic data acquisition and processing were carried out by Yun-bao Sun and Zhi-lei Sun. Horizon interpretation was completed by Ang Li and Dong Zhang. All authors participated in the field investigations, discussed the results and contributed to the final manuscript.

Declaration of competing interest

The authors declare no conflicts of interest.

Acknowledgement

This study was funded by the Geological Survey Program of the China Geological Survey (DD20230402, DD2026032030) and the National Natural Science Foundation of China (42072069).

References

Bangs NLB, Hornbach MJ, Berndt C, Alves TM. 2011. The mechanics of intermittent methane venting at South Hydrate Ridge inferred from 4D seismic surveying. Earth and Planetary Science Letters, 310(1–2), 105–112. doi: 10.1016/j.epsl.2011.06.022.

Bao X, Ji JQ, Tao T, Zhou LH, Wang JD, Fu LX, Yuan SQ. 2010. The structural features of X-shaped conjugate normal fault in seismic data and its significance in oil exploration. Chinese Journal of Geology, 45(2), 395–410 (in Chinese with English abstract).

Briais A, Patriat P, Tapponnier P. 1993. Updated interpretation of magnetic anomalies and seafloor spreading stages in the South China Sea: Implications for the Tertiary tectonics of Southeast Asia. Journal of Geophysical Research: Solid Earth, 98(B4), 6299–6328. doi: 10.1029/92JB02280.

Cai ZR, Liu WL, Wan ZF, Guo F. 2010. Determination of Cenozoic tectonic movement in the northern South China Sea and the relationship between oil-gas reservoir and tectonic movement. Marine Science Bulletin, 29(2), 161–165 (in Chinese with English abstract). doi: 10.11840/j.issn.1001-6392.2010.2.024.

Chen J, Hao HJ, Lin HM. 2002. Quality improvement of seismic data and new identification of Mesozoic prospects in Chaoshan Depression. China Offshore Oil and Gas (Geology), 16(4), 271–278 (in Chinese with English abstract).

Collett TS, Johnson AH, Knapp CC, Boswell R. 2009. Natural gas hydrates: A review. AAPG Memoir, 89, 146–219. doi: 10.1306/13201142M891602.

Ding WW, Wang YM, Chen HL, Yang SF, Wu NY. 2004. Deformation characters and its tectonic evolution of the Southwest Taiwan Basin. Journal of Zhejiang University (Science Edition), 31(2), 216–220 (in Chinese with English abstract). doi: 10.3321/j.issn:1008-9497.2004.02.023.

Ding WW, Li JB, Li J. 2010. Forming mechanism of the submarine canyon on the north slope of the South China Sea. Journal of Marine Sciences, 28(1), 26–31 (in Chinese with English abstract). doi: 10.3969/j.issn.1001-909X.2010.01.004.

Du XD, Liu J, Xu LY, Zhang QL, Zheng JY, Zhang M, Wu QL, Cai GF, Li SZ, Suo YH. 2021. The Dongsha movement in the Jieyang Sag at the northern South China Sea margin: Control on hydrocarbon traps. Geotectonica et Metallogenia, 45(1), 201–210 (in Chinese with English abstract). doi: 10.16539/j.ddgzyckx.2021.01.018.

Fan CY, Xia SH, Zhao F, Sun JL, Cao JH, Xu HL, Wan KY. 2017. New insights into the magmatism in the northern margin of the South China Sea: Spatial features and volume of intraplate seamounts. Geochemistry, Geophysics, Geosystems, 18(6), 2216–2239. doi: 10.1002/2016GC006792.

Gao YD, Liu J, Peng GR, Chen L, Wang ZY, Shi YL. 2024. New fields and resource potential of oil and gas exploration in Pearl River Mouth Basin. Acta Petrolei Sinica, 45(1), 183–201 (in Chinese with English abstract). doi: 10.7623/syxb202401011.

Gao YD, Xiang XD, Zhang XD. 2021. Cenozoic sedimentary evolution and its geological significance for hydrocarbon exploration in the northern South China Sea. Natural Gas Geoscience, 32(5), 645–656 (in Chinese with English abstract). doi: 10.11764/j.issn.1672-1926.2021.03.008.

He YL, Liang JQ, Kuang ZG, Deng W, Ren JF, Lai HF, Meng MM, Zhang W. 2022. Migration and accumulation characteristics of natural gas hydrates in the uplifts and their slope zones in the Qiongdongnan Basin, China. China Geology, 5(2), 234–250. doi: 10.31035/cg2022004.

Huang CY, Xia KY, Yuan PB, Chen PG. 2001. Structural evolution from Paleogene extension to Latest Miocene-Recent arc-continent collision offshore Taiwan: Comparison with on land geology. Journal of Asian Earth Sciences, 19(5), 619–638. doi: 10.1016/s1367-9120(00)00065-1.

Hustoft S, Mienert J, Bünz S, Nouzé H. 2007. High-resolution 3D-seismic data indicate focussed fluid migration pathways above polygonal fault systems of the mid-Norwegian margin. Marine Geology, 245(1–4), 89–106. doi: 10.1016/j.margeo.2007.07.004.

Laurent D, Gay A, Baudon C, Berndt C, Soliva R, Planke S, Mourgues R, Lacaze S, Pauget F, Mangue M, Lopez M. 2012. High-resolution architecture of a polygonal fault interval inferred from geomodel applied to 3D seismic data from the Gjallar Ridge, Vøring Basin, Offshore Norway. Marine Geology, 332, 134–151. doi: 10.1016/j.margeo.2012.07.016.

Li CF, Zhou ZY, Hao HJ, Chen HJ, Wang JL, Chen B, Wu JS. 2008. Late Mesozoic tectonic structure and evolution along the present-day northeastern South China Sea continental margin. Journal of Asian Earth Sciences, 31(4–6), 546–561. doi: 10.1016/j.jseaes.2007.09.004.

Li PL. 1993. Cenozoic tectonic movement in the Pearl River mouth basin. China Offshore Oil and Gas (Geology), 7(6), 11–17 (in Chinese with English abstract).

Li PL. 1994. Structural features and oil-and-gas accumulation in Pearl River Mouth Basin. Guangdong Geology, 9(4), 21–28 (in Chinese with English abstract).

Li SZ, Cao XZ, Wang GZ, Liu B, Li XY, Suo YH, Jiang ZX, Guo LL, Zhou J, Wang PC, Zhu JJ, Wang G, Zhao SJ, Liu YJ, Zhang GW. 2019. Meso-Cenozoic tectonic evolution and plate reconstruction of the Pacific plate. Journal of Geomechanics, 25(5), 642–677 (in Chinese with English abstract). doi: 10.12090/j.issn.1006-6616.2019.25.05.060.

Liang JQ, Zhang W, Lu J, Wei JG, Kuang ZG, He YL. 2019. Geological occurrence and accumulation mechanism of natural gas hydrates in the eastern Qiongdongnan Basin of the South China Sea: Insights from site GMGS5-W9-2018. Marine Geology, 418, 106042. doi: 10.1016/j.margeo.2019.106042.

Lin CS, Chu FY, Gao JY, Tan YH. 2007. On tectonic movement in the South China Sea during the Cenozoic. Acta Oceanologica Sinica, 29(4), 87–96 (in Chinese with English abstract). doi: 10.3321/j.issn:0253-4193.2007.04.010.

Liu J, Yang R, Zhang JH, Wei W, Wu DD. 2019. Gas hydrate accumulation conditions in the Huaguang Depression of Qiongdongnan Basin and prediction of favorable zones. Marine Geology & Quaternary Geology, 39(1), 134–142 (in Chinese with English abstract). doi: 10.16562/j.cnki.0256-1492.2018072701.

Liu JL, Wang SH, Yan W. 2015. Research on coexistence between marine gas hydrate and deepwater oil. Journal of Tropical Oceanography, 34(2), 39–51 (in Chinese with English abstract). doi: 10.11978/j.issn.1009-5470.2015.02.006.

Long GS, Shi HS, Zheng RC, Du JY, Chen SH, Ge YZ. 2011. Characteristics and development controlling factors of Paleogene deep reservoirs in Huizhou depression, Pearl River mouth basin. Marine Origin Petroleum Geology, 16(3), 71–78 (in Chinese with English abstract). doi: 10.3969/j.issn.1672-9854.2011.03.010.

Lu YT, Luan XW, Lyu FL, Wang B, Yang ZL, Yang TT, Yao GS. 2017. Seismic evidence and formation mechanism of gas hydrates in the Zhongjiannan Basin, Western margin of the South China Sea. Marine and Petroleum Geology, 84, 274–288. doi: 10.1016/j.marpetgeo.2017.04.005.

Lu YT, Xu XY, Luan XW, Jiang S, Ran WM, Yang TT, Lyu FL, Zhou YF, Yang ZL. 2021. Morphology, internal architectures, and formation mechanisms of mega-pockmarks on the northwestern South China Sea margin. Interpretation, 9(4), T1039–T1054. doi: 10.1190/int-2020-0175.1.

Lüdmann T, Kin Wong H, Wang PX. 2001. Plio–Quaternary sedimentation processes and neotectonics of the northern continental margin of the South China Sea. Marine Geology, 172(3–4), 331–358. doi: 10.1016/S0025-3227(00)00129-8.

Ostanin I, Anka Z, di Primio R, Bernal A. 2012. Identification of a large Upper Cretaceous polygonal fault network in the Hammerfest basin: Implications on the reactivation of regional faulting and gas leakage dynamics, SW Barents Sea. Marine Geology, 332, 109–125. doi: 10.1016/j.margeo.2012.03.005.

Ren JF, Qiu HJ, Kuang ZG, Li TW, He YL, Xu MJ, Wang XX, Lai HF, Liang J. 2024. Deep-large faults controlling on the distribution of the venting gas hydrate system in the middle of the Qiongdongnan Basin, South China Sea. China Geology, 7(1), 36–50. doi: 10.31035/cg2023086.

Ren JS, Chen TY, Niu BG, Liu ZG, Liu FR. 1990. Evolution of Tectonic Magmatism and Mineralization Laws in Eastern China Part 5: Structural Evolution and Mineralization of Continental Lithosphere in Eastern China and Adjacent Areas. Beijing, Science Press (in Chinese).

Shao L, You HQ, Hao HJ, Wu GX, Qiao PJ, Lei YC. 2007. Petrology and depositional environments of Mesozoic strata in the northeastern South China Sea. Geological Review, 53(2), 164–169 (in Chinese with English abstract). doi: 10.16509/j.georeview.2007.02.004.

Sun QL, Alves TM, Zhao MH, Sibuet JC, Calvès G, Xie XN. 2020. Post-rift magmatism on the northern South China Sea margin. Geological Society of America Bulletin, 132(11–12), 2382–2396. doi: 10.1130/b35471.1.

Sun QL, Wu SG, Lü FL, Yuan SQ. 2010. Polygonal faults and their implications for hydrocarbon reservoirs in the southern Qiongdongnan Basin, South China Sea. Journal of Asian Earth Sciences, 39(5), 470–479. doi: 10.1016/j.jseaes.2010.04.002.

Tang XY, Hu SB, Zhang GC, Liang JS, Yang SC, Shen HL, Rao S, Li WW. 2014. Geothermal characteristics and hydrocarbon accumulation of the northern marginal basins, South China Sea. Chinese Journal of Geophysics, 57(1), 64–78 (in Chinese with English abstract). doi: 10.1002/cjg2.20084.

Wang PC, Li SZ, Suo YH, Guo LL, Wang GZ, Hui GG, Santosh M, Somerville ID, Cao XZ, Li Y. 2020. Plate tectonic control on the formation and tectonic migration of Cenozoic basins in northern margin of the South China Sea. Geoscience Frontiers, 11(4), 1231–1251. doi: 10.1016/j.gsf.2019.10.009.

Wang XX, Cai F, Sun ZL, Li Q, Li A, Yan GJ, Sun YB, Luo D, Dong G. 2021. Sedimentary evolution and geological significance of the Dongsha submarine canyon in the northern South China Sea. Earth Science, 46(3), 1023–1037 (in Chinese with English abstract). doi: 10.3799/dqkx.2020.277.

Wei JG, Liang JQ, Lu JG, Zhang W, He YL. 2019. Characteristics and dynamics of gas hydrate systems in the northwestern South China Sea-Results of the fifth gas hydrate drilling expedition. Marine and Petroleum Geology, 110, 287–298. doi: 10.1016/j.marpetgeo.2019.07.028.

Wei XD, Ruan AG, Zhao MH, Qiu XL, Li JB, Zhu JJ, Wu ZL, Ding WW. 2011. A wide-angle OBS profile across Dongsha Uplift and Chaoshan Depression in the mid-northern South China Sea. Chinese Journal of Geophysics, 54(12), 3325–3335 (in Chinese with English abstract). doi: 10.3969/j.issn.0001-5733.2011.12.030.

Wu GX, Wang RJ, Hao HJ, Shao L. 2007. Microfossil evidence for development of marine Mesozoic in the north of South China Sea. Marine Geology & Quaternary Geology, 27(1), 79–85 (in Chinese with English abstract). doi: 10.16562/j.cnki.0256-1492.2007.01.010.

Xia B, Cui XJ, Xie JH, Wang R. 2004. Thinking about the dynamics mechanism study on formation and evolution of South China Sea. Geotectonica et Metallogenia, 28(3), 221–227 (in Chinese with English abstract). doi: 10.16539/j.ddgzyckx.2004.03.001.

Xie XN, Zhang C, Ren JY, Yao BC, Wan L, Chen H, Kang B. 2011. Effects of distinct tectonic evolutions on hydrocarbon accumulation in northern and southern continental marginal basins of South China Sea. Chinese Journal of Geophysics, 54(12), 3280–3291 (in Chinese with English abstract). doi: 10.3969/j.issn.0001-5733.2011.12.026.

Xie XN, Ren JY, Pang X, Lei C, Chen H. 2019. Stratigraphic architectures and associated unconformities of Pearl River Mouth Basin during rifting and lithospheric breakup of the South China Sea. Marine Geophysical Research, 40(2), 129–144. doi: 10.1007/s11001-019-09378-6.

Xie ZY, Sun LT, Pang X, Zheng JY, Sun Z. 2017. Origin of the Dongsha event in the South China Sea. Marine Geophysical Research, 38(4), 357–371. doi: 10.1007/s11001-017-9321-8.

Xie ZY, Wei JG, Zheng JY, Sun Z, Zhang K. 2022. A 3D basin modeling study of the factors controlling gas hydrate accumulation in the Shenhu Area of the South China Sea. China Geology, 5(2), 218–233. doi: 10.31035/cg2022012.

Ye JL, Wei JG, Liang JQ, Lu JG, Lu HL, Zhang W. 2019. Complex gas hydrate system in a gas chimney, South China Sea. Marine and Petroleum Geology, 104, 29–39. doi: 10.1016/j.marpetgeo.2019.03.023.

You KH, DiCarlo D, Flemings PB. 2015. Quantifying hydrate solidification front advancing using method of characteristics. Journal of Geophysical Research: Solid Earth, 120(10), 6681–6697. doi: 10.1002/2015JB011985.

Zhang W, Liang JQ, Su PB, Wei JG, Gong YH, Lin L, Liang J, Huang W. 2019. Distribution and characteristics of mud diapirs, gas chimneys, and bottom simulating reflectors associated with hydrocarbon migration and gas hydrate accumulation in the Qiongdongnan Basin, northern slope of the South China Sea. Geological Journal, 54(6), 3556–3573. doi: 10.1002/gj.3351.

Zhao SJ, Wu SG, Shi HS, Dong DD, Chen DX, Wang Y. 2012. Structures and dynamic mechanism related to the Dongsha movement at the northern margin of South China Sea. Progress in Geophysics, 27(3), 1008–1019 (in Chinese with English abstract). doi: 10.6038/j.issn.1004-2903.2012.03.022.

Zhong GJ, Zhang RW, Yi H, Feng CM, Zhao ZQ. 2018. The characteristics of shallow gas reservoir developed in the northern continental slope of South China Sea. Journal of Tropical Oceanography, 37(3), 80–85 (in Chinese with English abstract). doi: 10.11978/2017075.

Zhong GJ, Yan P, Sun M, Yu JH, Feng CM, Zhao J, Yi H, Zhao ZQ. 2020. Accumulation model of gas hydrate in the Chaoshan Depression of South China Sea, China. IOP Conference Series: Earth and Environmental Science, 569(1), 012070. doi: 10.1088/1755-1315/569/1/012070.

Zhong GJ, Su PB, Feng CM, Liu S, Sun M, YI H, Zhao J, Zhao ZQ. 2022. Mesozoic tectonic characteristics and exploration prospects of the Chaoshan depression in the northeastern South China Sea. Acta Geologica Sinica, 96(8), 2896–2905 (in Chinese with English abstract). doi: 10.19762/j.cnki.dizhixuebao.2022158.

Zhou D, Ru K, Chen HZ. 1995. Kinematics of Cenozoic extension on the South China Sea continental margin and its implications for the tectonic evolution of the region. Tectonophysics, 251(1–4), 161–177. doi: 10.1016/0040-1951(95)00018-6.